

Boron segregation and electrical properties in polycrystalline $\text{Si}_{1-x-y}\text{Ge}_x\text{C}_y$ and $\text{Si}_{1-y}\text{C}_y$ alloys

E. J. Stewart,^{a)} M. S. Carroll,^{b)} and J. C. Sturm

Center for Photonics and Optoelectronic Materials, Department of Electrical Engineering,
Princeton University, New Jersey 08544

(Received 3 July 2003; accepted 29 December 2003)

In this article, we report strong boron segregation to polycrystalline $\text{Si}_{1-x-y}\text{Ge}_x\text{C}_y$ from polysilicon during thermal anneals in the temperature range of 800–900 °C. This effect is larger than previous reports of segregation to single-crystal $\text{Si}_{1-x}\text{Ge}_x$ and increases with carbon concentration. Segregation also occurs in polycrystalline $\text{Si}_{1-y}\text{C}_y$, revealing that carbon by itself can drive the segregation (without germanium present). This segregation is used to model the enhanced threshold voltage stability of *p*-channel metal oxide semiconductor field effect transistors with boron-doped polycrystalline $\text{Si}_{1-x-y}\text{Ge}_x\text{C}_y$ gates. We also study the electrical properties of polycrystalline $\text{Si}_{1-x-y}\text{Ge}_x\text{C}_y$. For low carbon concentrations (0.4%), polycrystalline $\text{Si}_{1-x-y}\text{Ge}_x\text{C}_y$ has a similar level of dopant activation and mobility as polycrystalline $\text{Si}_{1-x}\text{Ge}_x$; increasing the concentration to 1.6% results in significant losses in both. Annealing the films for time scales similar to those needed for segregation causes no degradation of the electrical properties, indicating that electrically inactive defects are not driving the segregation. © 2004 American Institute of Physics.
[DOI: 10.1063/1.1649452]

I. INTRODUCTION

$\text{Si}_{1-x-y}\text{Ge}_x\text{C}_y$ and $\text{Si}_{1-y}\text{C}_y$ alloys are of great interest for controlling dopant diffusion in silicon-based devices, as well as for band-gap and strain engineering. The ability of carbon to reduce boron diffusion in single-crystal $\text{Si}_{1-x}\text{Ge}_x$ has been exploited to make high performance $\text{Si}/\text{Si}_{1-x-y}\text{Ge}_x\text{C}_y/\text{Si}$ heterojunction bipolar junction transistors;^{1,2} other potential applications include metal oxide semiconductor field effect transistor (MOSFET) channels and source/drains.^{3,4}

Polycrystalline $\text{Si}_{1-x-y}\text{Ge}_x\text{C}_y$ has also been studied as a gate electrode for *p*-channel MOSFETs. Conventional *p*-channel MOSFETs with heavily boron-doped polysilicon gates can suffer from threshold voltage instabilities, caused by boron diffusion from the gate through the gate oxide and into the channel during the post-implant anneal.⁵ Devices with polycrystalline $\text{Si}_{1-x-y}\text{Ge}_x\text{C}_y$ layers in the gate have less boron penetration, and greater threshold voltage stability, than devices with polycrystalline Si or $\text{Si}_{1-x}\text{Ge}_x$ gate layers.^{6,7} Boron accumulates in the polycrystalline $\text{Si}_{1-x-y}\text{Ge}_x\text{C}_y$ gate layers, reducing boron diffusion through the oxide and into the substrate. In this article, we study this segregation effect in detail, including its dependence on carbon content, germanium, and annealing conditions. To examine the possibility that carbon-related defects are driving the segregation, we investigate the effect of carbon on the electrical properties of polycrystalline Si and $\text{Si}_{1-x}\text{Ge}_x$, especially their stability with annealing. We then discuss the application of polycrystalline $\text{Si}_{1-x-y}\text{Ge}_x\text{C}_y$ to MOSFET gates

by modeling what effect the segregation has on threshold voltage stability.

II. EXPERIMENTAL DETAILS

All samples used in this study were grown by rapid thermal chemical vapor deposition, using germane, methylsilane, and diborane as sources for germanium, carbon, and boron, respectively. Polycrystalline $\text{Si}_{1-x-y}\text{Ge}_x\text{C}_y$ and $\text{Si}_{1-y}\text{C}_y$ layers were grown using silane and disilane as silicon sources, respectively, at 625 °C; polysilicon was deposited using either silane at 700 °C or disilane at 625 °C. Previous work shows that for single-crystal $\text{Si}_{1-x-y}\text{Ge}_x\text{C}_y$ and $\text{Si}_{1-y}\text{C}_y$ films grown under similar conditions as those used for this study, most of the carbon is substitutional.^{8,9} All layers were grown on thermally oxidized silicon substrates. Grain sizes in the polycrystalline $\text{Si}_{1-x-y}\text{Ge}_x\text{C}_y$ layers, from plan-view transmission electron microscopy (TEM), were observed to be about ~40 nm. Two types of structures were grown to study segregation in polycrystalline $\text{Si}_{1-x-y}\text{Ge}_x\text{C}_y$. The first was a two-layer structure consisting of a ~100 nm lightly *in situ* doped polycrystalline $\text{Si}_{0.765}\text{Ge}_{0.22}\text{C}_{0.015}$ layer followed by a 300 nm heavily *in situ* doped polysilicon layer. The second was a multilayer structure consisting of several 50 nm polycrystalline $\text{Si}_{1-x-y}\text{Ge}_x\text{C}_y$ layers (Ge=20%, carbon percentages varied from 0 to 1%) sandwiched between 70 nm polysilicon layers. All layers were *in situ* doped with boron at about 10^{20} cm^{-3} . Both of these samples were annealed at temperatures between 800 and 900 °C in N_2 to allow boron to move from the polysilicon layers into the polycrystalline $\text{Si}_{1-x-y}\text{Ge}_x\text{C}_y$ layers. An additional sample was grown to study segregation in polycrystalline $\text{Si}_{1-y}\text{C}_y$, containing two *in situ* doped ($[\text{B}] \sim 7 \times 10^{20}\text{ cm}^{-3}$) polycrystalline $\text{Si}_{1-y}\text{C}_y$ layers (carbon percentages=0.4 and 1%)

^{a)}Present address: Northrop Grumman Electronic System, Baltimore, MD; electronic mail Eric.J.Stewart@ngc.com

^{b)}Present address: Sandia National Laboratories, Albuquerque, NM.

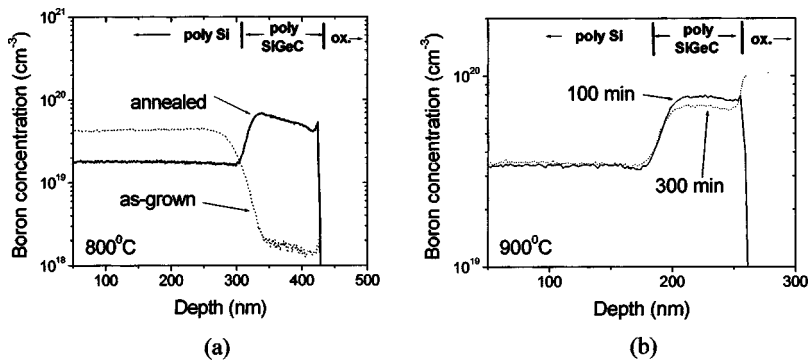


FIG. 1. SIMS profiles of boron concentration vs depth for the two-layer polycrystalline $\text{Si}/\text{Si}_{0.765}\text{Ge}_{0.22}\text{C}_{0.015}$ samples after (a) an 800°C , 44 h anneal,²⁴ and (b) 900°C anneals for 100 and 300 min.

sandwiched between polysilicon layers. This sample was annealed at 800°C for 22 h in N_2 to allow for boron redistribution. Secondary ion mass spectroscopy (SIMS) analysis was used to measure the germanium, carbon, and boron profiles in all samples.

III. BORON SEGREGATION TO POLYCRYSTALLINE $\text{Si}_{1-x-y}\text{Ge}_x\text{C}_y$ AND $\text{Si}_{1-y}\text{C}_y$

Boron segregation to polycrystalline $\text{Si}_{1-x-y}\text{Ge}_x\text{C}_y$ is clearly demonstrated in the two-layer polycrystalline $\text{Si}/\text{Si}_{0.765}\text{Ge}_{0.22}\text{C}_{0.015}$ structure. Figure 1(a) shows SIMS profiles of this structure before and after an 800°C , 44 h anneal. Before the anneal, the polysilicon layer is heavily doped at a level of $4 \times 10^{19} \text{cm}^{-3}$, while the polycrystalline $\text{Si}_{0.765}\text{Ge}_{0.22}\text{C}_{0.015}$ layer is lightly doped at a level of $2 \times 10^{18} \text{cm}^{-3}$. If there were no segregation between the layers, this profile would be expected to flatten out during the anneal. However, after annealing, boron levels have risen in the polycrystalline $\text{Si}_{0.765}\text{Ge}_{0.22}\text{C}_{0.015}$ layer to $4.6 \times 10^{19} \text{cm}^{-3}$, while boron concentration has decreased in the polysilicon to $1.5 \times 10^{19} \text{cm}^{-3}$, demonstrating strong segregation to the polycrystalline $\text{Si}_{0.765}\text{Ge}_{0.22}\text{C}_{0.015}$. Defining a segregation coefficient m as the ratio of boron concentration in the polycrystalline $\text{Si}_{1-x-y}\text{Ge}_x\text{C}_y$ to the polysilicon at the interface, we find $m=4.0$ for these parameters ($\text{Ge}=22\%$, $\text{C}=1.5\%$) and annealing conditions.

Figure 1(b) shows an example of boron segregation and its time dependence at 900°C . A similar structure (identical to previous sample except slightly thinner) was annealed for 100 and 300 min. After 100 min, segregation can again be seen, but is somewhat less than at 800°C ($m=2.4$). After 300 min of annealing, no increase in the segregation is observed. In fact, there appears to be a slight decrease (perhaps

due to the out-diffusion of carbon and germanium from the polycrystalline $\text{Si}_{1-x-y}\text{Ge}_x\text{C}_y$ layer into the polysilicon), but it is not known if this decrease is statistically significant. This indicates that anneal times on the order of 900°C for 100 min are long enough for the segregation process to occur.

The multilayer polycrystalline $\text{Si}_{1-x-y}\text{Ge}_x\text{C}_y$ structure shows that the segregation is strongly dependent on carbon level. SIMS of this structure before and after an 800°C , 18 h anneal are shown in Fig. 2(a). Before the anneal, the polycrystalline $\text{Si}_{1-x-y}\text{Ge}_x\text{C}_y$ layers are *in situ* doped slightly higher than the polysilicon layers. This was unintentionally done during growth (due to the different deposition conditions for polycrystalline $\text{Si}_{1-x-y}\text{Ge}_x\text{C}_y$ versus polysilicon— 625 versus 700°C , respectively), and is not attributable to a segregation effect. Without segregation, however, this profile would be expected to flatten out during the anneal. In the polycrystalline $\text{Si}_{1-x-y}\text{Ge}_x\text{C}_y$ layers with high carbon levels (0.5 and 1%), however, the boron concentration actually increases during the anneal, revealing segregation to these layers. In the layers with carbon levels of 0.0 and 0.05%, boron concentrations are below their initial values, leaving open the possibility that the peaks simply remain due to slow out-diffusion. However, given previous reports of diffusion in polycrystalline $\text{Si}_{1-x}\text{Ge}_x$,¹⁰ these anneal conditions should be sufficient to allow for complete out-diffusion, making the remaining peaks most likely due to segregation. In Fig. 3, the segregation coefficients as a function of carbon percentage are presented. Segregation to polycrystalline $\text{Si}_{0.8}\text{Ge}_{0.2}\text{C}_y$ was observed (consistent with previous reports of segregation to single-crystal $\text{Si}_{1-x}\text{Ge}_x$ Refs. 11 and 12), but was weak ($m=1.1$). It then steadily increases for carbon concentrations up to 1%. Also plotted are segregation coefficients for the

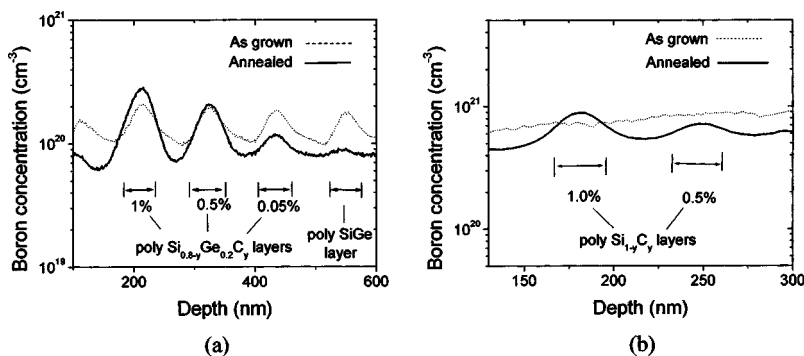


FIG. 2. SIMS profiles of boron concentration vs depth for (a) the multilayer polycrystalline $\text{Si}_{0.8-y}\text{Ge}_{0.2}\text{C}_y$ sample annealed at 800°C for 18 h and (b) the multilayer polycrystalline $\text{Si}_{1-y}\text{C}_y$ sample annealed at 800°C for 22 h.

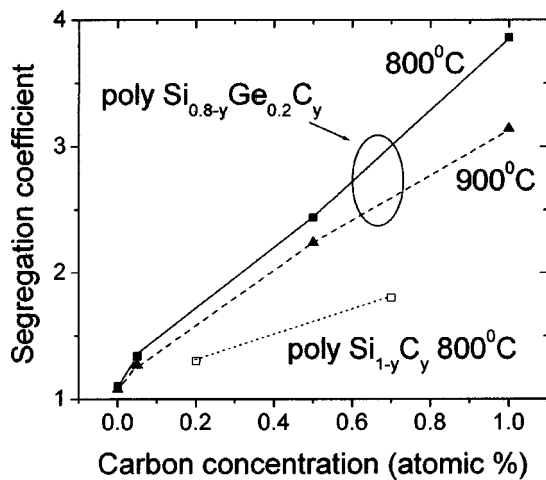


FIG. 3. Segregation coefficients vs carbon concentration for the multilayer polycrystalline $\text{Si}_{0.8-y}\text{Ge}_{0.2}\text{C}_y$ (annealed at 800°C for 18 h or 900°C for 100 min) and $\text{Si}_{1-y}\text{C}_y$ (annealed at 800°C for 22 h) samples.

same sample subjected to a 900°C 100 min anneal (instead of 800°C), showing again reduced segregation at higher temperature. Further annealing at 900°C showed no increase in segregation for this sample as well, consistent with the two-layer case. Assuming an activation energy for boron diffusion of ~ 3.5 eV (an upper estimate for boron diffusion in polysilicon), anneal times at 800°C of 18 h should also be long enough to allow for complete segregation (for layers of similar thickness). Therefore we can assume that in Fig. 2(a) there has also been enough time to establish a quasi-equilibrium between the layers.

The polycrystalline $\text{Si}_{1-y}\text{C}_y$ multilayer structure demonstrates that carbon by itself can cause segregation, without germanium present. Figure 2(b) shows SIMS profiles of this sample before and after annealing. Boron segregates to the polycrystalline $\text{Si}_{1-y}\text{C}_y$ layers, with coefficients of 1.3 and 1.8 for layers which had initial carbon fractions of 0.4 and 1.0%, respectively. These coefficients, however, are somewhat lower compared to polycrystalline $\text{Si}_{1-x-y}\text{Ge}_x\text{C}_y$ layers with similar values. One difference we observe is that the out-diffusion of carbon from the polycrystalline $\text{Si}_{1-y}\text{C}_y$ layers is faster than from the polycrystalline $\text{Si}_{1-x-y}\text{Ge}_x\text{C}_y$ layers (Fig. 4). After the anneal, the peak carbon percentages have decreased to 0.2 and 0.7%, respectively, in the polycrystalline $\text{Si}_{1-y}\text{C}_y$ sample. In the polycrystalline $\text{Si}_{1-x-y}\text{Ge}_x\text{C}_y$ sample, carbon concentrations remained close

to their initial values for the high carbon concentrations (1 and 0.5%). Therefore in Fig. 3 we plot the segregation coefficients for the polycrystalline $\text{Si}_{1-y}\text{C}_y$ layers versus the final carbon concentrations, not the initial values. Nevertheless, the segregation coefficients are still lower than in the polycrystalline $\text{Si}_{1-x-y}\text{Ge}_x\text{C}_y$ layers. Since the peak doping levels in this sample are significantly higher than in the polycrystalline $\text{Si}_{1-x-y}\text{Ge}_x\text{C}_y$ sample ($7 \times 10^{20} \text{ cm}^{-3}$ versus $2 \times 10^{20} \text{ cm}^{-3}$), a strict comparison is difficult, making it hard to quantify the germanium effect (For example, boron clustering may be having an effect on the redistribution process¹³).

IV. ELECTRICAL PROPERTIES

A separate set of samples was used to investigate the electrical properties of boron-doped polycrystalline $\text{Si}_{1-x-y}\text{Ge}_x\text{C}_y$ layers. Single layers of *in situ* doped polycrystalline Si, $\text{Si}_{1-x}\text{Ge}_x$, and $\text{Si}_{1-x-y}\text{Ge}_x\text{C}_y$ ($\text{Ge}=25\%$, thicknesses ranged from 150 to 300 nm) were grown on thermally oxidized (~ 200 nm) Si substrates. Growth conditions were the same as in the previous section, with doping levels ranging from 10^{18} to 10^{21} cm^{-3} and carbon levels ranging from 0 to 1.6%. All samples were annealed at 900°C for times similar to or longer than those used to study segregation in the previous section. This was done to examine what effect the segregation process may be having on the electrical properties (i.e., possible formation of inactive boron-carbon defects). Boron and carbon levels were determined by SIMS, and resistivity, dopant activation, and mobility measurements were taken using the four point probe and Van der Pauw techniques at room temperature.

Figure 5 shows the as-deposited (no annealing) dopant activation and mobility for polycrystalline $\text{Si}_{1-x-y}\text{Ge}_x\text{C}_y$ samples doped at a level of $2 \times 10^{19} \text{ cm}^{-3}$, as a function of carbon content. The same silane, germane, and diborane flows were used for all three samples; only the methylsilane flow was varied for the different carbon levels. Boron concentrations were measured by SIMS measurements, and showed that the boron incorporation is not significantly affected by the methylsilane flow. Polycrystalline $\text{Si}_{1-x}\text{Ge}_x$ (no carbon) has a resistivity of $7.6 \times 10^{-2} \text{ ohm cm}$ and mobility of $7.1 \text{ cm}^2/\text{V s}$, comparable to previous reports at these doping levels.¹⁰ Polysilicon samples (doped at $1 \times 10^{19} \text{ cm}^{-3}$, not shown) had similar dopant activation but lower mobilities ($2.9 \text{ cm}^2/\text{V s}$). When low carbon concentrations (0.4%)

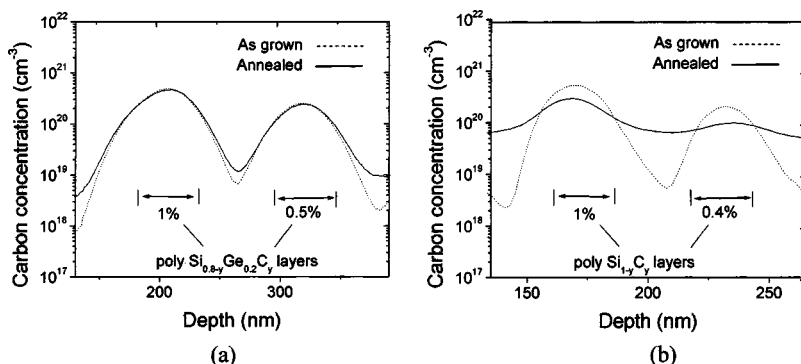


FIG. 4. SIMS profiles of carbon concentration vs depth for (a) the multilayer polycrystalline $\text{Si}_{0.8-y}\text{Ge}_{0.2}\text{C}_y$ sample annealed at 800°C for 18 h and (b) the multilayer polycrystalline $\text{Si}_{1-y}\text{C}_y$ sample annealed at 800°C for 22 h.

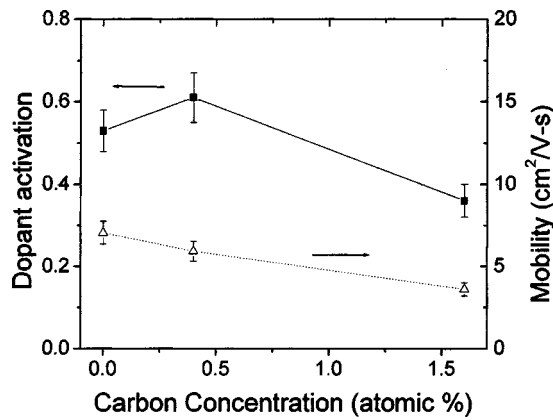


FIG. 5. Dopant activation and mobility as a function of carbon concentration for the as-grown (no annealing) polycrystalline $\text{Si}_{0.75-y}\text{Ge}_{0.25}\text{C}_y$ single-layer samples doped with boron at $2 \times 10^{19} \text{ cm}^{-3}$.

are added to polycrystalline $\text{Si}_{1-x}\text{Ge}_x$, there is a slight increase in hole concentration, but the change is less than the error bars of the measurement. There was also a small decrease in the mobility (17%). As the carbon level is increased to 1.6%, however, significant losses in both dopant activation (32%) and mobility (49%) versus the polycrystalline $\text{Si}_{1-x}\text{Ge}_x$ sample are observed.

The electrical properties are fairly stable with annealing. Figure 6 shows resistivity, dopant activation, and mobility versus annealing at 900°C for the $2 \times 10^{19} \text{ cm}^{-3}$ doped samples from Fig. 5 (the polysilicon sample doped at $1 \times 10^{19} \text{ cm}^{-3}$ is also included). Dopant activation remains

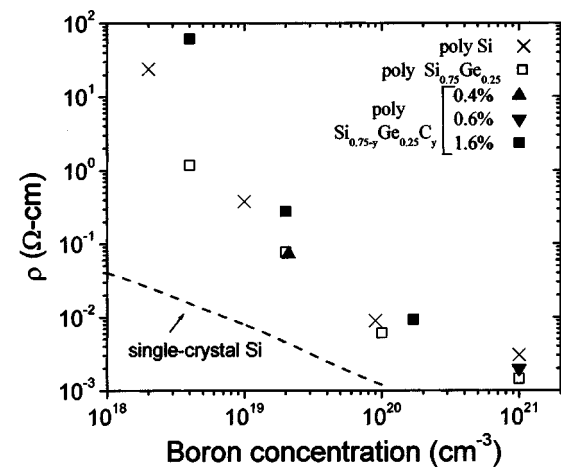


FIG. 7. Resistivity vs boron concentration (from SIMS) for polycrystalline Si, $\text{Si}_{0.8}\text{Ge}_{0.2}$, and $\text{Si}_{0.8-y}\text{Ge}_{0.2}\text{C}_y$ samples. Also shown is the data for single-crystal silicon (dotted line) from Ref. 18.

mostly flat for all annealing times and carbon levels. Mobilities increase at first, presumably due to increases in grain size, and then stabilize. As a result, resistivities initially decrease and then level off. Resistivity measurements (although not Hall measurements to find mobility) were also taken out to 24 h of annealing, and remained stable.

Figure 7 shows the resistivity of the as-grown samples as a function of doping concentration. For low carbon levels (0.4% at 10^{19} doping and 0.6% at 10^{21} doping), polycrystalline $\text{Si}_{1-x-y}\text{Ge}_x\text{C}_y$ resistivities are similar to those of the polycrystalline $\text{Si}_{1-x}\text{Ge}_x$. However, for the high carbon lev-

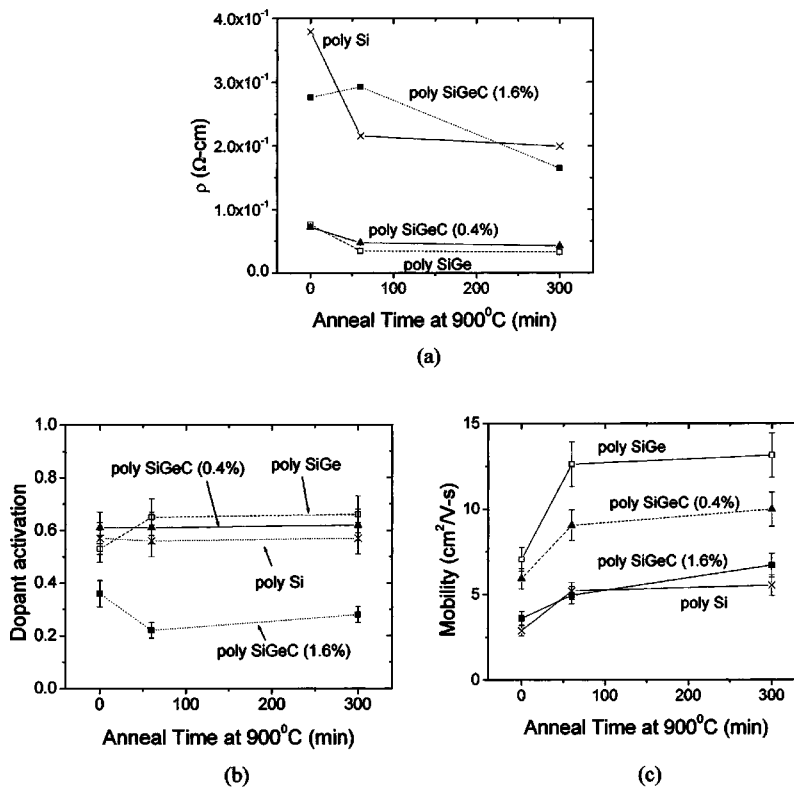


FIG. 6. (a) Resistivity, (b) dopant activation, and (c) mobility as a function of anneal time at 900°C for the polycrystalline $\text{Si}_{0.75-y}\text{Ge}_{0.25}\text{C}_y$ single-layer samples doped at $2 \times 10^{19} \text{ cm}^{-3}$. Also included are the measurements for polysilicon doped at $1 \times 10^{19} \text{ cm}^{-3}$.

els (1.6%), they are larger over the entire range of doping. The magnitude of this increase depends on doping level: it is largest at low doping ($\sim 50\times$ at 10^{18} cm^{-3}) and smaller at higher doping ($\sim 2.5\times$ at 10^{20} cm^{-3}). Long anneals (900 °C for several hours) were performed over all doping levels and, similar to Fig. 6, the electrical properties were very stable.

When small amounts of carbon (less than 2%) are added to single-crystal silicon or $\text{Si}_{1-x}\text{Ge}_x$, most reports have found that (for boron doping) dopant activation is not affected, but mobilities decrease by factors ranging from 11–60%.^{14–16} The mobility drop has been attributed to increased scattering due to the presence of the carbon, either by electrically active defects or alloy scattering.

Conduction in polycrystalline material is different from the single-crystal case due to carrier trapping at grain boundaries. In polycrystalline silicon, grain boundaries introduce large numbers of states close to the middle of the energy gap.¹⁷ These can effectively trap majority carriers. As a result, the grain boundaries become charged and potential barriers form, which impede the flow of charged carriers between grains and reduce the effective mobility. This becomes worse as the grain size is reduced or the trap density is increased. At low doping levels, the grain boundaries can trap a large fraction of the carriers and the potential barriers become very high, so the resistivity is very high. As the doping level is increased, the potential barriers become narrower and lower, and a smaller fraction of carriers are trapped, so the conductivity approaches that of single-crystal Si. Our overall results are consistent with these models. At the 10^{18} doping level, the polysilicon resistivity is several orders of magnitude higher than in single-crystal. Resistivity decreases rapidly as boron concentration is increased above this level, and approaches single-crystal values (with similar doping) in the 10^{20} – 10^{21} range (for comparison, the single-crystal resistivity is plotted versus boron doping in Fig. 7¹⁸).

Boron-doped polycrystalline $\text{Si}_{1-x}\text{Ge}_x$ is known to have lower resistivity than polysilicon.^{10,19} This difference has been attributed to a larger grain size and a shift of the trap states toward the valence band, resulting in less carrier trapping and an increased mobility. Our results are consistent with these observations as well, with our polycrystalline $\text{Si}_{1-x}\text{Ge}_x$ samples (doped at the $2\times 10^{19}\text{ cm}^{-3}$ level) having about 2.5 times higher mobility than polysilicon [Fig. 6(c)].

Our as-deposited polycrystalline $\text{Si}_{1-x-y}\text{Ge}_x\text{C}_y$ samples (Fig. 5) with low carbon concentration (0.4%) have similar dopant activation and only a slightly decreased mobility compared to polycrystalline $\text{Si}_{1-x}\text{Ge}_x$. The mobility decrease may be due to the previously mentioned carbon-induced scattering seen in single-crystal films with similar carbon levels. This retention of most of the electrical properties of polycrystalline $\text{Si}_{1-x}\text{Ge}_x$ makes low-carbon polycrystalline $\text{Si}_{1-x-y}\text{Ge}_x\text{C}_y$ attractive for device applications, such as MOSFET gates. However, the high carbon concentrations (1.6%) see a large decrease both in carrier activation and mobility. This was seen in one previous article and attributed to an increase in the trap density at the grain boundaries caused by carbon.²⁰ An increased trap density would trap a much larger fraction of the active carriers, reducing the carrier concentration, and form larger potential barriers, re-

ducing the mobility. For the growth conditions used for these layers, at carbon levels above 1% some of the carbon may be incorporating on nonsubstitutional sites during growth, and perhaps more readily form these traps. The fact that resistivity increases more rapidly with decreasing doping level (Fig. 7) for the 1.6% polycrystalline $\text{Si}_{1-x-y}\text{Ge}_x\text{C}_y$ layer (versus polysilicon or polycrystalline $\text{Si}_{1-x}\text{Ge}_x$) is consistent with the carrier trapping model. At low doping, a difference in trap density will have a larger effect on the resistivity because a larger fraction of the carriers are being trapped, and the potential barriers are more sensitive to the trap density. However, it cannot be ruled out that some sort of B–C defect is being incorporated as-grown in the grain and directly rendering the boron inactive.

V. DISCUSSION OF SEGREGATION AND DEVICE IMPLICATIONS

The stability of the electrical properties with annealing provides insight into the mechanism of boron segregation. One potential driving mechanism is that boron is becoming trapped at a carbon-related defect. For example, silicon carbide (SiC) precipitates are known to form in $\text{Si}_{1-x-y}\text{Ge}_x\text{C}_y$ layers with similar carbon levels and annealing conditions,^{21,22} and boron could become immobilized either inside or at the surfaces of these defects. A direct interaction between boron and carbon might also be occurring, such as the B–C–I cluster proposed by Liu *et al.*²³ Either of these defects might be expected to render the boron electrically inactive. This should be detectable by the electrical measurements in the single-layer polycrystalline $\text{Si}_{1-x-y}\text{Ge}_x\text{C}_y$ films—as they are annealed and given time to form B–C defects, one would expect to see a loss in the concentration of electrically active boron. However, as shown in Fig. 6(b), this is not observed. In particular, for the polycrystalline $\text{Si}_{0.746}\text{Ge}_{0.25}\text{C}_{0.004}$ sample, no loss in dopant activation is observed as a function of annealing. Thus boron is not moving to electrically inactive sites. For this carbon concentration, however, under the same annealing conditions, significant boron segregation is observed. This argues against boron-carbon defects or defect complexes as the driving force for boron segregation to polycrystalline $\text{Si}_{1-x-y}\text{Ge}_x\text{C}_y$ from Si. In other work involving single-crystal material, we will present evidence that gradients of silicon interstitials, created by substitutional carbon, can drive boron segregation to $\text{Si}_{1-x-y}\text{Ge}_x\text{C}_y$ layers from Si.

As mentioned in the introduction, *p*-channel MOSFETs with polycrystalline $\text{Si}_{1-x-y}\text{Ge}_x\text{C}_y$ layers in the gate are less susceptible to boron penetration than devices with polysilicon or $\text{Si}_{1-x}\text{Ge}_x$ gate layers. Boron accumulates in the polycrystalline $\text{Si}_{1-x-y}\text{Ge}_x\text{C}_y$ layers, with less penetrating through the gate oxide and into the channel. These devices thus have greater threshold voltage stability. Here, using the segregation data presented in this paper together with the structures from the previous study,⁷ we quantitatively model this effect. In particular, we investigate two questions: (i) Is the segregation observed here powerful enough to reduce boron penetration as found in the previous work, and (ii) What happens as the carbon level is varied in the polycrystalline $\text{Si}/\text{Si}_{1-x-y}\text{Ge}_x\text{C}_y$ gate?

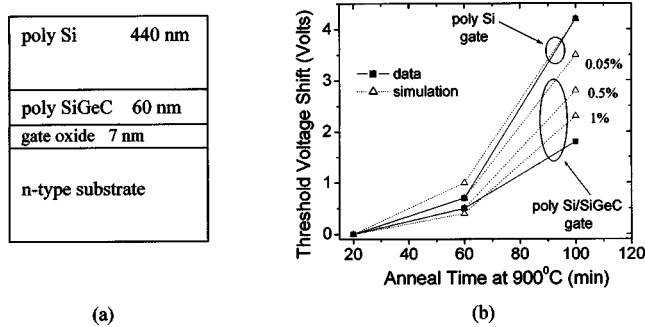


FIG. 8. Simulation results of PMOS devices with polycrystalline $\text{Si}/\text{Si}_{1-x-y}\text{Ge}_x\text{C}_y$ gates, showing (a) the structures used in both the previous study⁷ and the simulations in this work, and (b) the threshold voltage shifts vs anneal time, with solid symbols and lines representing data from the previous work (for the polycrystalline $\text{Si}/\text{Si}_{1-x-y}\text{Ge}_x\text{C}_y$ sample, the carbon content was 0.35%), and open symbols and dotted lines the results of simulations performed in this work.

Using the Tsurpem4 simulator, we modeled the PMOS devices from the previous study with either all polysilicon gates or polycrystalline $\text{Si}/\text{Si}_{1-x-y}\text{Ge}_x\text{C}_y$ gates [Fig. 8(a)]. All structures consisted of n -type substrate ($1 \times 10^{15} \text{ cm}^{-3}$), 7-nm gate oxide, and 500 nm total gate thickness. The experimental (and simulated) process conditions consisted of a 60 keV BF_2^+ implant at $2 \times 10^{15} \text{ cm}^{-2}$, followed by a post-implant anneal in N_2 at 900 °C for either 20, 60, or 100 min. The threshold voltages of the modeled boron profiles were extracted for the different anneal times and plotted in Fig. 8(b). First, the model parameters were adjusted to fit the data for the control (polysilicon gate) sample. The effective diffusivity in the polysilicon was set to $7.5 \times 10^{-13} \text{ cm}^2/\text{s}$ to match our diffusion profiles during the 20 min anneal. Then, the boron diffusivity in the gate oxide was increased by a factor of 74 to model the fluorine enhancement effect (due to BF_2^+ implant⁵), to match the threshold voltage shift we observe for the 100 min anneal time. It can be seen that the all polysilicon-gated devices experience large positive threshold voltage shifts caused by boron out-diffusion from the gate [Fig. 8(b)].

For the simulation of the polycrystalline $\text{Si}/\text{Si}_{1-x-y}\text{Ge}_x\text{C}_y$ structure, a boron segregation coefficient was introduced between the polycrystalline $\text{Si}_{1-x-y}\text{Ge}_x\text{C}_y$ and polysilicon. No changes in diffusivity were assumed. The segregation coefficient caused boron to pile up in the polycrystalline $\text{Si}_{1-x-y}\text{Ge}_x\text{C}_y$ layer versus the polycrystalline Si; in addition, it reduced boron segregation into the oxide by the same amount (this is a key assumption necessary to see the reduced boron penetration). Carbon levels of 0.05, 0.5, and 1% were modeled using coefficients at 900 °C taken from Fig. 3 ($m = 1.27, 2.23, \text{ and } 3.14$, respectively), and the results plotted in Fig. 8(b). The simulations show that the segregation strongly suppresses boron out-diffusion, noticeable even at carbon levels of only 0.05%. Larger effects are seen at carbon levels of 0.5 and 1.0%. If the simulated results are compared to the experimental results for the polycrystalline $\text{Si}/\text{Si}_{1-x-y}\text{Ge}_x\text{C}_y$ gate (by linearly interpolating the segregation values for 0.35% carbon), we find that the simulation predicts improved threshold voltage stability, but

not as much as in experiment. Additional effects, such as a reduced boron diffusivity in the polycrystalline $\text{Si}_{1-x-y}\text{Ge}_x\text{C}_y$, may be playing a role. We conclude from this analysis that higher carbon levels (at least up to 1%) should result in increased resistance to boron penetration for devices with polycrystalline $\text{Si}/\text{Si}_{1-x-y}\text{Ge}_x\text{C}_y$ gates. However, as shown in Fig. 5, high carbon concentrations will eventually degrade the conductivity of the polycrystalline $\text{Si}_{1-x-y}\text{Ge}_x\text{C}_y$ layers, resulting in a potential tradeoff between gate conductivity and threshold voltage stability.

VI. SUMMARY

In summary, we find that boron segregates from polycrystalline Si to polycrystalline $\text{Si}_{1-x-y}\text{Ge}_x\text{C}_y$ layers with carbon contents up to 1%. Anneal times on the order of hours at 900 °C are long enough for the segregation to take place. Segregation to polycrystalline $\text{Si}_{1-y}\text{C}_y$ layers shows that carbon by itself can drive the segregation. Polycrystalline $\text{Si}_{1-x-y}\text{Ge}_x\text{C}_y$ layers with low carbon concentrations (0.4%) show no significant loss in mobility or carrier activation versus polycrystalline $\text{Si}_{1-x}\text{Ge}_x$, while at higher concentrations (1.6%) significant reductions are observed. These reductions, however, are less severe at higher doping levels. The stability of the electrical properties with annealing indicates that boron atoms are not being deactivated during anneals due to carbon-related defects. Further work is in progress to directly check for SiC precipitation in these films using TEM. Simulations of PMOS structures show that increasing the carbon level in a polycrystalline $\text{Si}_{1-x-y}\text{Ge}_x\text{C}_y$ gate layer should result in increased ability to suppress boron penetration and the threshold voltage instabilities that result.

ACKNOWLEDGMENTS

This work was supported by DARPA and ARO.

- ¹L. D. Lanzerotti, J. C. Sturm, E. Stach, R. Hull, T. Buyuklimanli, and C. Magee, *Appl. Phys. Lett.* **70**(23), 3125 (1997).
- ²H. J. Osten, D. Knoll, B. Heinemann, and P. Schley, *IEEE Trans. Electron Devices* **46**(9), 1910 (1999).
- ³I. Ban, M. C. Ozturk, and E. K. Demirlioglu, *IEEE Trans. Electron Devices* **44**(9), 1544 (1997).
- ⁴E. Napolitani, A. Coati, D. De Salvador, A. Carnera, S. Mirabella, S. Scalse, and F. Priolo, *Appl. Phys. Lett.* **79**(25), 4145 (2001).
- ⁵J. R. Pfister, F. K. Baker, T. C. Mele, H. Tseng, P. J. Tobin, J. D. Hayden, J. W. Miller, C. D. Gunderson, and L. C. Parrillo, *IEEE Trans. Electron Devices* **37**(8), 1842 (1990).
- ⁶C. L. Chang and J. C. Sturm, *Appl. Phys. Lett.* **74**(17), 2501 (1999).
- ⁷E. J. Stewart, M. S. Carroll, and J. C. Sturm, *IEEE Electron Device Lett.* **22**(12), 574 (2001).
- ⁸C. W. Liu, A. St. Amour, J. C. Sturm, Y. R. J. Lacroix, M. L. W. Thewalt, C. W. Magee, and D. Eaglesham, *J. Appl. Phys.* **80**(5), 3043 (1996).
- ⁹M. S. Carroll and J. C. Sturm, *Appl. Phys. Lett.* **81**(7), 1225 (2002).
- ¹⁰C. Salm, D. T. van Veen, D. J. Gravesteijn, J. Holleman, and P. H. Woerlee, *J. Electrochem. Soc.* **144**(10), 3665 (1997).
- ¹¹S. M. Hu, D. C. Ahlgren, P. A. Ronsheim, and J. O. Chu, *Phys. Rev. Lett.* **67**(11), 1450 (1991).
- ¹²T. T. Fang, W. T. C. Fang, P. B. Griffin, and J. D. Plummer, *Appl. Phys. Lett.* **68**(6), 791 (1996).
- ¹³S. Solmi, E. Landi, and F. Baruffaldi, *J. Appl. Phys.* **68**(7), 3250 (1990).
- ¹⁴H. J. Osten, G. Lippert, P. Gaworzewski, and R. Sorge, *Appl. Phys. Lett.* **71**(11), 1522 (1997).
- ¹⁵H. J. Osten and P. Gaworzewski, *J. Appl. Phys.* **82**(10), 4977 (1997).
- ¹⁶T. Noda, D. Lee, H. Shim, M. Sakuraba, T. Matsuura, and J. Murota, *Thin Solid Films* **380**, 57 (2000).

- ¹⁷T. I. Kamins, *J. Appl. Phys.* **42**(11), 4357 (1971).
- ¹⁸S. M. Sze, *Physics of Semiconductor Devices* (Wiley, New York, 1981) p. 32.
- ¹⁹T.-J. King, J. P. McVittie, K. C. Saraswat, and J. R. Pfiester, *IEEE Trans. Electron Devices* **41**(2), 228 (1994).
- ²⁰I. M. Anteney, G. J. Parker, P. Ashburn, and H. A. Kemhadjian, *J. Appl. Phys.* **90**(12), 6182 (2001).
- ²¹L. V. Kulik, D. A. Hits, M. W. Dashiell, and J. Kolodzey, *Appl. Phys. Lett.* **72**(16), 1972 (1998).
- ²²P. Warren, J. Mi, F. Overney, and M. Dutoit, *J. Cryst. Growth* **157**, 414 (1995).
- ²³C.-L. Liu, W. Windl, L. Borucki, S. Lu, and X.-Y. Liu, *Appl. Phys. Lett.* **80**(1), 52 (2002).
- ²⁴E. J. Stewart, M. S. Carroll, and J. C. Sturm, *MRS Symposium Proceedings*, **669**, paper J6.9 (2001).